Overview of the characteristic features of the magnetic phase transition with regards to the magnetocaloric effect: the hidden relationship between hysteresis and latent heat

Overview of the characteristic features of the magnetic phase transition with regards to the magnetocaloric effect: the hidden relationship between hysteresis and latent heat

K. Morrison[1] and L.F. Cohen[2]

[1]*Department of Physics, Loughborough University, Loughborough, LE11 3TU, UK*

[2]*The Blackett Laboratory, Imperial College, London SW7 2BZ, UK*

The magnetocaloric effect has seen a resurgence in interest over the last 20 years as a means towards an alternative energy efficient cooling method. This has resulted in a concerted effort to develop the so-called “giant” magnetocaloric materials with large entropy changes that often come at the expense of hysteretic behaviour. But do the gains offset the disadvantages? In this paper we review the relationship between the latent heat of several giant magnetocaloric systems and the associated magnetic field hysteresis. We quantify this relationship by the parameter $\Delta\mu_0 H/\Delta S_L$, which describes the linear relationship between field hysteresis, $\Delta\mu_0 H$, and entropy change due to latent heat, ΔS_L. The general trends observed in these systems suggest that itinerant magnets appear to consistently show large ΔS_L accompanied by small $\Delta\mu_0 H$ ($\Delta\mu_0 H/\Delta S_L$ = 0.02 ± 0.01 T/(J.K^{-1}kg^{-1})), compared to local moment systems, which show significantly larger $\Delta\mu_0 H$ as ΔS_L *increases* ($\Delta\mu_0 H/\Delta S_L$ = 0.14 ± 0.06 T/(J.K^{-1}kg^{-1})).

I. Introduction

In magnetic materials the application of a magnetic field under adiabatic conditions can result in heating due to the magnetocaloric effect, where a reduction in magnetic entropy results in an increase of lattice entropy. This suggests the possibility of a cyclic process to achieve cooling, a technology that has the advantages of an absence of greenhouse gases and a potential increase in engine system efficiency compared to conventional vapour compression systems.[1] Whilst utilisation of the magnetocaloric effect was proposed by Debye[2] and Giauque[3] for cooling below 1 K in the early 20th century, it was not until the seminal papers by Brown[4], and Pecharsky and Gschneidner[5] that room temperature magnetic refrigeration started to be considered a viable application.

Almost two decades on, there are now a handful of materials that have been identified as suitable candidates for solid state refrigeration. For the most part these material systems are described as exhibiting a Giant Magnetocaloric Effect (GMCE); typically defined as an entropy change that exceeds that of the standard benchmark material, Gd. A common feature of such GMCE materials is magneto-volume or magneto-structural coupling that results in field and thermal hysteresis, an example of which can be found in $Gd_5(Ge_{1-x}Si_x)_4$. In this material system, an appropriate choice of Si content (x=0.5) produces an orthorhombic to monoclinic structural transition that coincides with a ferromagnetic (FM) to paramagnetic (PM) transition.[6] Whilst the entropy change at this field driven phase transition is promising (ΔS ~ 15 $J.K^{-1}.kg^{-1}$), this magnitude of entropy change requires large operating fields (~ 2-5 T) and the system shows significant field hysteresis ($\Delta\mu_0 H$ ~ 1 T). In order to develop future attractive materials for use in a commercial solid-state refrigeration device, a compromise needs to be reached between the magnitude of ΔS, the required magnetic field, material fatigue, and hysteretic losses.

In this paper the general characteristics of the phase transition in a collection of material systems considered interesting with regards to applications of the magnetocaloric effect will be discussed. The magneto-volume, structural and elastic coupling in these material systems that leads to a moderate or giant magnetocaloric effect will also be considered in light of the associated detrimental hysteresis and its relationship with the development of latent heat.

II. Experimental

The full details of preparation routes for each of the samples discussed in this paper are reported elsewhere. Single crystal $Gd_5Ge_2Si_2$ was prepared by the Bridgman method;[7] $DyCo_2$ was prepared by arc melting;[8] the $La(Fe,Si)_{13}$ bulk ingots were prepared by arc melting followed by annealing at 1323 K for 7 days; the $Co(Mn_{1-x}Fe_x)(Si_{1-y}Ge_y)$ alloys were prepared by induction melting followed by annealing at 1223 K;[9] $Mn_{1.95}SbCr_{0.05}$ was prepared by arc melting;[10] $La_{0.67}Ca_{0.33}MnO_3$ and $RMnO_3$ were prepared by standard solid state methods.[11,12]

Magnetisation measurements were carried out using a Quantum Design vibrating sample magnetometer (VSM) for temperatures ranging from 77 K to 300 K and at a field sweep rate of 0.5 T/min.

Microcalorimetry measurements were obtained for 100 μm fragments using a commercial Xensor (TCG-3880) SiN membrane gauge that has been adapted to work as an ac calorimeter[13] or an adiabatic temperature probe[14] in a cryostat capable of 0 to 8 T and 4.2 to 295 K. (The sample size is typically limited to the size of the heater on the SiN chip: 50 x 100 μm.) As an ac calorimeter the heat capacity, C_p, is measured by application of an ac temperature modulation to the sample whilst held in He exchange gas. The solution to the heat transfer equation yields C_p of the sample as a function of the phase and amplitude of the resultant thermal modulation (with respect to the source signal). Due to the nature of the ac technique, it measures C_p alone, and not the latent heat, ΔQ_L. Whilst any latent heat that occurs on first driving the phase transition may be registered, as it is neither reversible nor necessarily in phase with the temperature modulation, it will not yield a repeatable measurement.[15] In order to fully sample the latent heat a separate measurement is required: the adiabatic temperature probe.[14] When operated in this mode the helium exchange gas is evacuated and the temperature change due to a change in applied magnetic field is registered. The noise floor of this measurement is of the order of 1 μV, which is equivalent to 1 nJ.

III. Characteristics of the continuous phase transition

The Ehrenfest classification of phase transitions defines the “order” of a phase transition by the order of the derivative after which the Gibbs function exhibits a discontinuity.[16] In a simple magnetic system the Gibbs function can be written as:

$$G = U - TS + \mu_0 HM \qquad (1)$$

where U is the internal energy, T the temperature, S the entropy, H the applied magnetic field, and M the magnetisation.

When Equation 1 is differentiated with respect to temperature (at constant field) we obtain:

$$\left(\frac{\partial G}{\partial T}\right)_H = \frac{\partial U}{\partial T} - T\frac{\partial S}{\partial T} + \mu_0 H \frac{\partial M}{\partial T} \qquad (2)$$

where the second term is equivalent to heat capacity and the third term is equivalent to the derivative of the magnetisation with respect to temperature. Thus, a discontinuity in the measurement of heat capacity (i.e. latent heat) is expected at a first order phase transition. In a similar way, the magnetisation as a function of temperature will present a discontinuity at a first order phase transition when differentiated with respect to temperature (or indeed field at fixed temperature). Higher order phase transitions would exhibit a discontinuity only when further differentiating with respect to field or temperature and are referred to here as 'continuous', the aim being to distinguish between systems with and without latent heat.

Gd was chosen to demonstrate the characteristics of a magnetocaloric (MC) material which exhibits a continuous phase transition. Due to an ordering temperature close to room temperature (T_c = 294 K), and a large magnetic moment (M_{sat}= 7.43 μ_B/Gd), this material is often used as a benchmark to compare other MC materials against.[17] Figure 1 shows some of the characteristic features of the phase transition, which includes:

1. A continuous change in magnetic moment,
2. Good agreement with the Curie-Weiss relationship for inverse susceptibility, and
3. Continuous changes in the heat capacity as a function of field.

It should be noted that whilst heat capacity measurements are often presented as a function of temperature we instead display them here with respect to field. This is in order to complement the latent heat data presented later. Also, for measurements close to room temperature, small changes in the heat capacity might be observed due to sample movement (see Figure 1(b) at 296 K) as the adhesion of the thermal grease used to fix the sample onto the membrane starts to decrease. This results in the small hysteresis observed in Figure 1(b) where it would otherwise not be expected.

IV. Mechanisms for the onset of the first order phase transition

For the majority of MC materials studied (normal magnetocaloric effect), the magnetic transition involves a paramagnetic (PM) to ferromagnetic (FM) change of state, which results in a change of magnetic entropy ($-|\Delta S_M|$). Due to conservation of entropy, under adiabatic conditions this decrease in magnetic entropy gives rise to a change of temperature ($+|\Delta T_{ad}|$). In the absence of volume effects and structural phase transitions, the PM-FM phase transition is expected to be continuous;[18] however this would limit the maximum achievable entropy change and thus the operating power of the 'refrigerant'. In order to maximise the achievable entropy change, efforts have been focussed on seeking a material that has one or more of the following:

1) A coupled structural transition (e.g. $Gd_5Ge_2Si_2$ changes from an orthorhombic FM to monoclinic PM[6]),
2) Strong magneto-elastic coupling (e.g. competing exchange interactions in CoMnSi,[19] or the Jahn-Teller distortion in manganites[20]),
3) An associated change in volume, i.e. magneto-volume coupling (e.g. $La(Fe,Si)_{13}$ exhibits a volume change, $\Delta V/V$, of ~1%[21]).

In each case, the energy barrier that results in a first order phase transition is due to some change in the crystal lattice that occurs alongside a magnetic change of state.[18]

The major advantage of the microcalorimetry technique presented here is that the first order characteristics of the phase transition (i.e. latent heat, ΔQ_L) can be separated from continuous changes in heat capacity. Whilst other techniques such as differential scanning calorimetry can be used to estimate ΔQ_L, this often also includes disorder broadening of the phase transition that makes it difficult to distinguish between the actual latent heat and gradual changes in the heat capacity *for complex phase transitions*. The size of the sample measured using this technique is one factor that limits the averaging effect of disorder broadening, another is the thermal modulation technique itself. Overall, this results in an independent measure of how much the total entropy change, ΔS_{tot}, increases as latent heat is introduced, whilst enabling correlation of ΔQ_L, with the observed hysteresis of the phase transition, $\Delta \mu_0 H$. When studying the material system in this way it will generally will fall under one of two cases (or a combination of the two), as outlined in the following sections.

IV. A. Case 1: Step-like changes in heat capacity.

For strong magneto-structural coupling, the change in magnetic moment is often sharp with respect to field or temperature. An example of such a first order phase transition is given in Figure 2. Here, the sample is single crystal $Gd_5Ge_2Si_2$, which exhibits a co-incident magnetic (FM-PM) and structural (orthorhombic-monoclinic) change of state in response to magnetic field or temperature. Although the bulk $M(H)$ loop shown in Figure 2(a) is broad with respect to field, Hall probe imaging of the surface confirmed that locally, the magnetic moment switches sharply.[22] This local change in moment is reflected in the latent heat data, $\Delta Q_{L,}$ of Figure 2(d), which indicates multiple nucleation(s) of FM phase over a range of critical fields. The corresponding change in heat capacity shown in Figure 2(c) exhibits a step-like change that occurs over the same field window as the latent heat, ΔQ_L. As a check of this measurement, we have compared measured values against independent data.

The latent heat contribution to the total entropy change at a given temperature, $\Delta S_L(T)$, can be obtained by finding the sum of ΔQ_L and dividing by temperature, T:

$$\Delta S_L(T) = \sum \frac{\Delta Q_L}{T} \qquad (3)$$

For the $Gd_5Ge_2Si_2$ single crystal this results in a value of ΔS_L = 6.39 ± 0.3 $J.K^{-1}.kg^{-1}$ at 285 K, compared to the total entropy change at this temperature of ΔS_{tot} = 12.5 ± 0.6 $J.K^{-1}.kg^{-1}$.[23] This value agrees well with the structural contribution determined by Liu *et al.*[24] and Pecharsky *et al.*[25] to be between 40 and 60% of ΔS_{tot}.

In contrast to the example of a continuous phase transition this first order phase transition shows:

1. A continuous change in bulk magnetic moment that is comprised of multiple sharp changes in the local magnetic moment (nucleation), with slightly different critical fields (Fig 2(a)).
2. A linear trend in the Curie-Weiss plot (inverse susceptibility) away from T_c, and then a departure from linearity with a sharp drop to zero at T_c (Fig. 2(b)), and
3. A step like change in the heat capacity accompanied by latent heat.

Typically, with Case 1 phase transitions the latent heat and change in heat capacity are only weakly dependant on temperature and where there are changes in the magnitude of the latent heat it is not directly reflected in the heat capacity.

IV. B. Case 2: Coupled heat capacity and latent heat behaviour.

Case 2 behaviour is typically observed in itinerant metamagnets where the first order phase transition is often signalled by S-shaped *M(H)* loops, as can be seen in Figure 3(a). One example of an itinerant metamagnet is the $LaFe_{13-x}Si_x$ material system, which exhibits volume changes of the order of 1% at T_c; it is this large volume change that leads to the energy barrier required for a first order phase transition.[18] As the silicon content (x) is decreased, the volume change increases and the phase transition becomes more first order. The result is an increase of the Curie temperature, T_c, with respect to the transition temperature in the absence of a volume change, T_0. (This corresponds to a divergence of the Curie-Weiss plot due to the volume change at the phase transition, as seen in Figure 3(b); a property that was highlighted by Bean and Rodbell in their work on magneto-volume driven first order phase transitions.[18])

As with the previous examples, the characteristic features of this type of phase transition include:

1. A continuous change in magnetic moment (Fig. 3(a)),
2. Divergence of the inverse susceptibility from the linear behaviour expected by the Curie-Weiss law (Fig. 3(b)), indicating two different Curie temperatures: T_o (in the absence of a volume change), and T_c (the observed Curie temperature), and
3. A large change in the heat capacity (ΔC>100%) accompanied by latent heat, both of which change dramatically with increasing temperature (Fig. 3(c)&(d)).

Typically with Case 2 phase transitions the field driven latent heat is sensitive to increasing temperature and this is also reflected in the change in heat capacity. Another example of this type of phase transition is the RCo_2 material system (where R is a rare earth);[26] similar features were observed for R=Dy.[8] In each case, as the temperature is increased the phase transition is driven towards continuous behaviour, where:

1. The hysteresis decreases,
2. The magnitude of the latent heat decreases (see arrow indicator in Fig. 3(d)), and

3. The amplitude of the heat capacity at the phase transition changes non-monotonically (see arrow indicators in Fig. 3(c)).

The shape of the heat capacity curve is also significantly different to both continuous and Case 1 phase transitions. For example, in Figure 3(c) a peak in C_p can be observed (that in a measurement that does not separate the contributions might be mistakenly attributed to latent heat) that moves to higher magnetic fields as the temperature is increased. Another important point to note is that the magnitude of the change in heat capacity is significantly larger for Case 2 phase transitions. In addition, these changes can exceed observations for continuous phase transitions (such as Gd in Figure 1(b)).

IV. C. Exceptions

Whilst the characteristics of the Case 1 and Case 2 first order phase transitions discussed in sections IV. A. and IV. B. were fairly straightforward, it is possible that other material systems may exhibit a combination of the two (characteristics). An example of this is the antiferromagnetic (AFM)-FM phase transition of CoMnSi (see Figure 4), which exhibits an inverse magnetocaloric effect[27] (cooling on field increase). Here, whilst the phase transition largely exhibits Case 1 characteristics, there are indicators of a precursor increase in the heat capacity, similar to that seen in Case 2. The phase transition is also particularly sensitive to changing temperature.

Disorder broadening[28] (of the phase transition) may also make it difficult to identify whether it is first order (or not). Whilst it is common to use the Banerjee criterion to determine whether a phase transition is first order, as this criterion is based on the mean field approximation it is likely to break down in the case of itinerant magnets where spin fluctuations may play a larger role.[8,12]

V. Hysteresis as a function of entropy gain

The relationship between $\Delta\mu_0 H$ *and* ΔS_L in different systems provides insight into the relationship between energy barriers and latent heat. Uniquely, the separation of entropy change due to latent heat, ΔS_L, and heat capacity, $\Delta S_{HC,}$ (where $\Delta S_{tot} = \Delta S_L + \Delta S_{HC}$), in fragments approaching the nucleation size of the phase transition enables determination of the parameter $\Delta\mu_0 H/\Delta S_L$, as shown in Figure 5. In this case, the hysteresis, $\Delta\mu_0 H$, was determined as the difference in applied magnetic field of features observed in latent heat measurements, and ΔS_L was determined using equation (3)

(or where the latent heat was distributed with respect to field, such as in Figure 3(d), the method outlined in references [8~~10~~] and [12~~14~~] was used). Whilst the effect of extrinsic hysteresis (due to temperature change or strain) has been mentioned elsewhere,[29] due to the limited size of the microcalorimetry samples this is often not a consideration. In either case, latent heat measurements were obtained for field sweep rates of 0.5 T/min and 0.1 T/min, which exhibited no significant difference in $\Delta\mu_0 H$ (therefore it can be assumed that the extrinsic hysteresis was negligible). Before discussing the general features of Figure 5 further, however, the potential impact of additional factors on the intrinsic hysteresis will be discussed.

In Figure 5(a), some results for the $CoMn_{1-x}Fe_xSi_{1-y}Ge_y$ alloy (which is sensitive to strain and has strong magnetocrystalline anisotropy), are shown. In this case, whilst each individual measurement followed a linear trend (aside from the Fe doped sample, which will be discussed later), it appears that the gradient of this line, $\Delta\mu_0 H/\Delta S_L$, was also sensitive to strain and field orientation. For example, by quenching the CoMnSi ingot after melting, strain is introduced that inhibits the phase transition. This results in an increase in $\Delta\mu_0 H/\Delta S_L$ of the quenched CoMnSi (quenched).[30] Additionally, as the size of the fragment measured in microcalorimetry is of the order of a single crystallite it is possible that this could be aligned according to the easy axis of magnetisation resulting in a decrease of $\Delta\mu_0 H/\Delta S_L$ (Ge doped).[31] Lastly, it was also shown that for the Fe doped CoMnSi at low temperatures the structural contribution to entropy change continues to increase whilst the magnetic entropy change has saturated. As these two contributions compete in this material system, this results in a decrease of the total entropy change, and indeed the latent heat, thus $\Delta\mu_0 H/\Delta S_L$ is no longer constant (Fe doped).[32] Overall, whilst these additional factors can influence the absolute value of $\Delta\mu_0 H/\Delta S_L$, each of these examples still followed a general linear trend.

In Figure 5(b) the $\Delta\mu_0 H(\Delta S_L)$ for a larger set of samples that exhibit Case 1 and Case 2 characteristics is shown. Notice that this data exhibits two (general) linear trends:

Case 1 - Where magneto-structural or magneto-exchange effects typically dominate, $\Delta\mu_0 H/\Delta S_L$ = 0.14 ± 0.06 $T.K.kg.J^{-1}$.

Case 2 - Where magneto-volume or magneto-elastic effects typically dominate, $\Delta\mu_0 H/\Delta S_L$ = 0.02 ± 0.01 $T.K.kg.J^{-1}$.

Note that the large error on the value of $\Delta\mu_0 H/\Delta S_L$ here is to encompass the selection of materials shown. This result suggests that although magneto-structural coupling could, in principle, lead to larger entropy changes, the associated hysteresis is significantly large. In particular, magneto-structural coupling appears to be less attractive in comparison to other routes of introducing first order behaviour, such as magneto-volume or magneto-elastic coupling: there is a fivefold increase of the value of $\Delta\mu_0 H/\Delta S_L$ for Case 1 phase transitions compared to Case 2 phase transitions.

VI. Conclusion

We have shown that for first order magnetic phase transitions the general characteristics can fall into one of two categories: Case 1, where magneto-structural coupling probably plays a large role and the latent heat is largely independent of temperature; and Case 2 where an itinerant metamagnetic phase transition occurs and the heat capacity and latent heat both change dramatically with temperature. Once identified, it appears that Case 1 phase transitions exhibit larger increases of $\Delta\mu_0 H$ with respect to ΔS_L, compared to Case 2 phase transitions ($\Delta\mu_0 H/\Delta S_L$ = 0.14 ± 0.06 T.K.kg.J^{-1} and 0.02 ± 0.01 T.K.kg.J^{-1}, respectively).

The results of this work indicate that the largest gain is to be had in itinerant magnets (that typically exhibit Case 2 characteristics), where spin fluctuations may play a role in lowering the energy barrier to the phase transition. An additional benefit is the ease with which they can be tuned with respect to field, temperature, or composition in order to approach the tri-critical point.[1] Overall, this suggests that material systems which exhibit an easily tunable critical point (i.e. where the phase transition moves from continuous to first order) are desirable not only because they enable better control of the desired properties (ΔS, ΔT_{ad}, and T_c), but also because of the lower hysteresis ($\Delta\mu_0 H$) associated with them.

Whilst the last 20 years have seen an increase in known material systems that exhibit favourable MC properties, the detrimental impact of hysteresis, durability and poor thermal conductivity are starting to become apparent.[33,34,35,36] This has resulted in a shift of focus towards material systems that lie closer to the critical point: on the cusp of first order and continuous phase transitions. As this technology approaches maturity it is reasonable to speculate that focus will continue to shift towards tri-critical magnets that can be easily shaped, react well with thermal engineering, and respond rapidly to changing magnetic field.

Acknowledgements

The authors would like to express their gratitude to the various individuals who provided us with good quality samples, without which this paper would not have been possible. In particular: T.A. Lograsso and Y. Mudryk of Ames Laboratory ($Gd_5Ge_2Si_2$, $DyCo_2$), K.G. Sandeman (CoMnSi based alloys), J. Lyubina and O. Gutfleisch ($La(Fe,Si)_{13}$), L. Caron ($Mn_{1.95}SbCr_{0.05}$), J. Turcaud ($La_{0.67}Ca_{0.33}MnO_3$) and A. Berenov ($RMnO_3$). LFC acknowledges funding for this work from EPSRC EP/G060940/1.

Figures

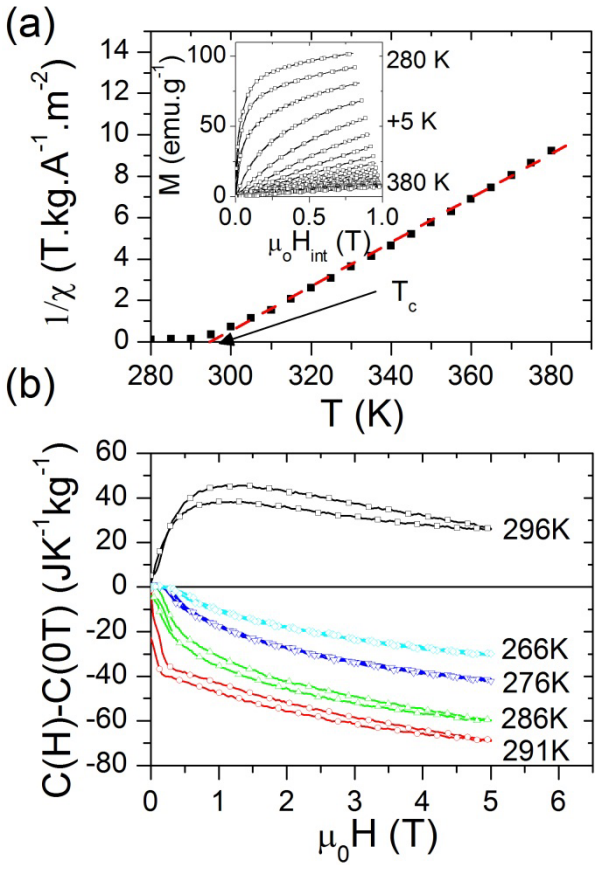

Figure 1 (a) Curie-Weiss plot for Gd determined from *M(H)* data as a function of temperature (shown in inset). (b) Change in heat capacity as a function of applied magnetic field. The apparent hysteresis observed here is due to sample movement, as discussed in text.

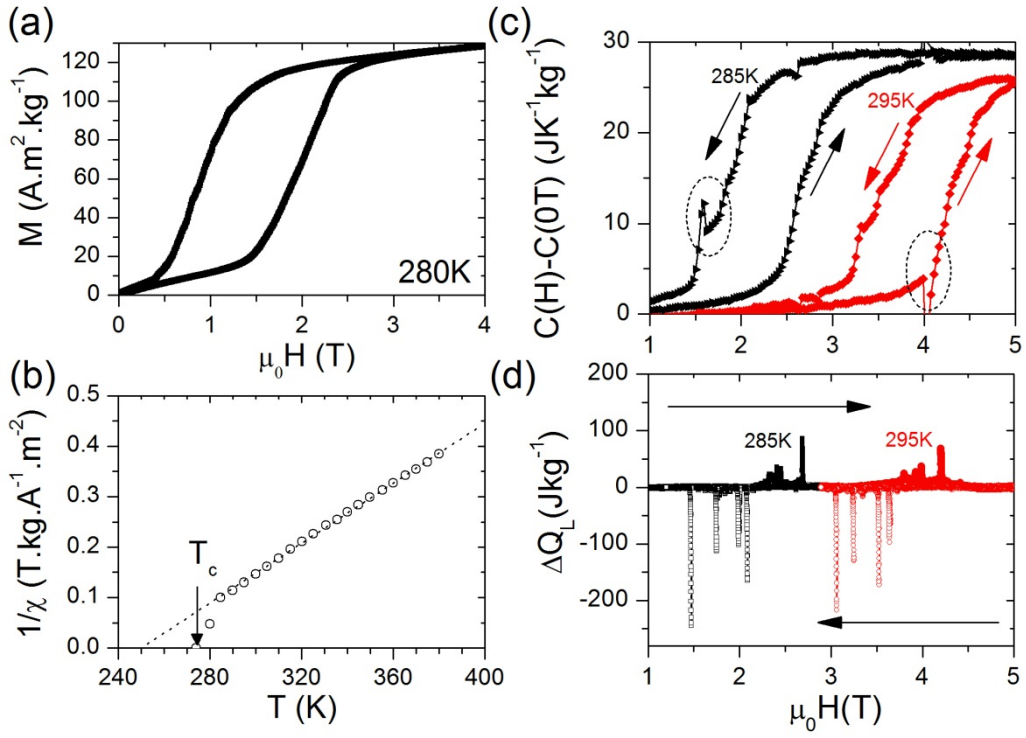

Figure 2 – (a) Typical *M(H)* loop for the $Gd_5Ge_2Si_2$ single crystal with (b) the corresponding Curie-Weiss plot as a function of temperature. (c)&(d) Microcalorimetry data taken for the $Gd_5Si_2Ge_2$ single crystal with the *b* axis aligned with the magnetic field. The arrows here indicate the direction of field sweep for each measurement. (c) Change in heat capacity as a function of field, where the dotted circles highlight small (irreproducible) artefacts due to latent heat. (d) Corresponding latent heat of the field-driven phase transition.

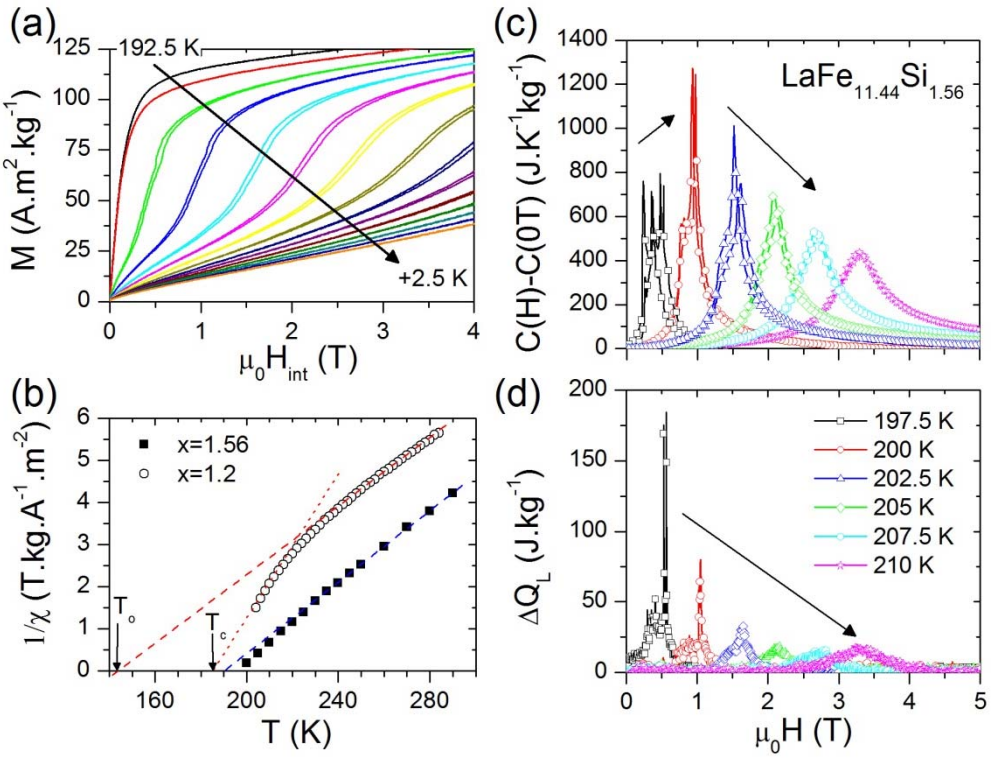

Figure 3 – (a) *M(H)* loops for $LaFe_{11.44}Si_{1.56}$ at increments of 2.5 K (where the S-shaped curve moves to higher fields as the temperature is increased, as indicated by the arrow), and (b) the corresponding Curie-Weiss plots for $LaFe_{11.44}Si_{1.56}$ and $LaFe_{11.8}Si_{1.2}$. Dashed lines indicate linear behaviour of the Curie-Weiss plot at temperatures far above T_c that were used to estimate T_o. The dotted line for x=1.2 indicates the linear behaviour of the Curie-Weiss plot close to T_c. (See text for details.) (c) Change in heat capacity and (d) latent heat measurements for $LaFe_{11.44}Si_{1.56}$, where the general trend(s) with regards to the magnitude of these measurements are indicated by arrows.

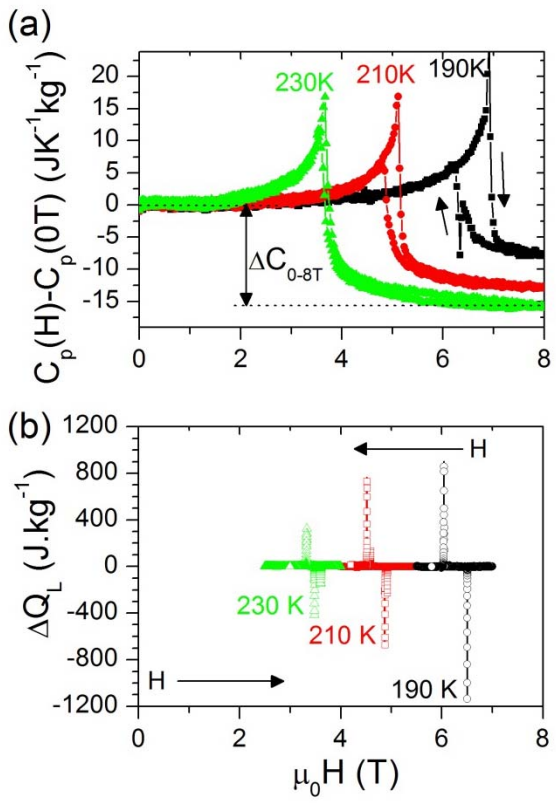

Figure 4 – (a) Change in heat capacity for $CoMnSi_{0.92}Ge_{0.08}$, which indicates both a step-like change in C_p (Case 1) as well as the signature (gradual) increase in C_p as the transition is approached (Case 2). The arrows on the data for 190 K indicate the direction of magnetic field sweep. (b) Corresponding latent heat data for $CoMnSi_{0.92}Ge_{0.08}$, where the arrows indicate the direction of field sweep. Notice that here the latent heat is negative on increasing magnetic field, unlike in Figures (2)&(3) where it was positive.

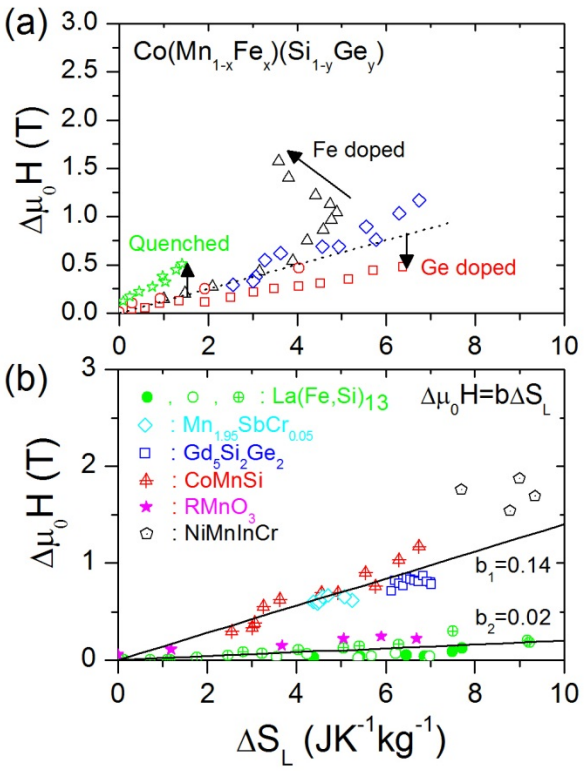

Figure 5 – Relationship between entropy change due to latent heat, ΔS_L, and hysteresis, $\Delta\mu_0 H$. (a) Impact of strain, fragmentation and anisotropy on the observed $\Delta\mu_0 H(\Delta S_L)$ relationship for the $Co(Mn_{1-x}Fe_x)(Si_{1-y}Ge_y)$ material system. (b) General trend(s) observed for the material systems presented here, where magneto-structural coupling (Case 1) leads to $\Delta\mu_0 H/\Delta S_L$ = 0.14 ± 0.06 T/(J.K^{-1}kg^{-1}) and magneto-elastic coupling in $La(Fe,Si)_{13}$ and $RMnO_3$ (Case2) leads to $\Delta\mu_0 H/\Delta S_L$ = 0.02 ± 0.01 T/(J.K^{-1}kg^{-1}).

References

[1] K.G. Sandeman: *Scripta Materialia, 2012, vol. 67, pp. 566-571*.
[2] P. Debye: *Ann. Phys., 1926, vol. 81, pp. 1154-1160*.
[3] W.F. Giauque and D.P. MacDougall: *Phys. Rev., 1933, vol. 43, pp. 768-768*.
[4] G.V. Brown: *J. Appl. Phys., 1976, vol. 47, pp. 3673-3680*.
[5] V.K. Pecharsky and K.A. Gschneidner, Jr.: *Phys. Rev. Lett., 1997, vol. 78, pp. 4494-4497.*
[6] V.K. Pecharsky and K.A. Gschneidner Jr.: *Adv. Mater., 2001, vol. 13, pp. 683-686*.
[7] H. Tang, A.O. Pecharsky, D.L. Schlagel, T.A. Lograsso, V.K. Pecharsky and K.A. Gschneidner, Jr.: *J. Appl. Phys. 2003, vol. 93, pp. 8298*. .
[8] K. Morrison, A. Dupas, A.D. Caplin, L.F. Cohen, Y. Mudryk, V.K. Pecharsky and K.A. Gschneidner: *Phys. Rev. B, 2013, vol 87, pp. 134421.*
[9] K.G. Sandeman, R. Daou, S. Özcan, J.H. Durrell, N.D. Mathur and D.J. Fray: *Phys. Rev. B, 2006, vol. 74, pp. 224436.*
[10] L. Caron, X.F. Miao, J.C.P Klaasse, S. Gama and E. Brück: arXiv:1307.3194 [cond-mat.mtrl-sci].
[11] K. Morrison, L.F. Cohen and A. Berenov: *Materials Research Society Symposium Proceedings, 2011, vol. 1310, pp. 31-40.*
[12] K. Morrison, M. Bratko, J. Turcaud, A.D. Caplin, L.F. Cohen and A. Berenov: *Rev. Sci. Instrum., 2012, vol. 83, pp.* 0034-6748.

[13] A.A. Minkaov, S.B. Roy, Y.V. Bugoslavsky and L.F. Cohen: *Rev. Sci. Instrum.*, *2005, vol. 76*, *pp. 043906.*
[14] Y. Miyoshi, K. Morrison, J.D. Moore, A.D. Caplin and L.F. Cohen: *Rev. Sci. Instrum., 2008, vol. 79, pp.* 074901.
[15] K. Morrison, J. Lyubina, K.G. Sandeman, L.F. Cohen, A.D. Caplin, J.D. Moore and O. Gutfleisch: Philosophical Magazine, 2012, vol. 92, pp. 292-303.
[16] C.J. Adkins: Equilibrium Thermodynamics, Third Edition, Cambridge University Press, 1983, pp. 180-205.
[17] K.A. Gschneidner Jr, V.K. Pecharsky and A O Tsokol: *Rep. Prog. Phys., 2005, col. 68, pp. 1479.*
[18] C.P. Bean and D.S. Rodbell: *Phys. Rev.*, *1962, vol. 126, pp. 104-115.*
[19] A. Barcza, Z. Gercsi, K. S. Knight and K. G. Sandeman: *Phys. Rev. B, 2010 vol. 104, pp. 247202*.
[20] H.A. Jahn and E. Teller: *Proc. R. Soc. Lond. A, 1937, vol. 161, pp. 220−235*.
[21] A. Fujita, Y. Akamatsu and K. Fukamichi: *J. App. Phys., 1999, vol. 86, pp. 4766-4768*.
[22] J.D. Moore, K. Morrison, G.K. Perkins, L.F. Cohen, D.L. Schlagel, T.A. Lograsso, K.A. Gschneidner, Jr. and V.K. Pecharsky: *Advanced Materials, 2009, vol. 21, pp. 3780-3783*.
[23] K. Morrison, L.F. Cohen, V.K. Pecharsky and K.A. Gschenidner, Jr.: *Materials Research Society Symposium Proceedings, 2011, vol. 1310, pp. 47-53.*
[24] G.J. Liu, J.R. Sun, J. Lin, Y.W. Xie, T.Y. Zhao, H.W. Zhang and B.G. Shen: *Appl. Phys. Lett., 2006, vol.* 88, pp. 212505.
[25] V.K. Pecharsky, K.A. Gschneidner, Jr., Ya. Mudryk and D. Paudyal, J. Magn. & Magn. Mater. 321, 3541-3547 (2009)
[26] E. Gratz and A.S. Markosyan: *J. Phys.: Condens. Matter, 2001, vol. 13, pp. R385-R413.*
[27] T. Krenke, E. Duman, M. Acet, E.F. Wassermann, X. Moya, L. Mañosa and A. Planes: *Nat. Mater., 2005, vol. 4, pp. 450-454.*
[28] Y. Imry and M. Wortis: *Phys. Rev. B, 1979, vol. 19, pp. 3580.*
[29] J.D. Moore, K. Morrison, K.G. Sandeman, M. Katter and L.F. Cohen: *Appl. Phys. Lett., 2009, vol. 95, 252504*.
[30] K. Morrison, J.D. Moore, K.G. Sandeman, A.D. Caplin, L.F. Cohen, A. Barcza, M.K. Chattopadhyay and S.B. Roy: *J. Phys. D: Appl. Phys, 2010, vol. 43, pp. 195001*.
[31] K. Morrison, J.D. Moore, K.G. Sandeman, A.D. Caplin and L.F. Cohen: *Phys. Rev. B, 2009, vol. 79, pp. 134408.*
[32] K. Morrison, Y. Miyoshi, J.D. Moore, A.D. Caplin, L.F. Cohen, A. Barcza and K.G. Sandeman: *Phys. Rev. B, 2008, vol. 78, pp. 134418.*
[33] J. Lyubina, R. Schäfer, N. Martin, L. Schultz and O. Gutfleisch: *Adv. Mater., 2010, vol. 22, pp. 3735-3739.*
[34] A. Smith, C.R.H. Bahl, R. Bjørk, K. Engelbrecht, K.K. Nielsen and N. Pryds: *Adv. Energy Mater., 2012, vol. 2, pp. 1288-1318.*
[35] J.A. Turcaud, K. Morrison, A. Berenov, N.McN. Alford, K.G. Sandeman and L.F. Cohen: *Scripta Materialia, 2013, vol. 68, pp. 510-513.*
[36] H. Zhang, Y.J. Sun, E. Niu, F.X. Hu, J.R. Sun and B.G. Shen: *Appl. Phys. Lett.,2014, vol. 104, pp. 062407.*